

Design of a CZT Gamma-Camera for GRB and Fast Transient Follow-up: a Wide-Field-Monitor for the EDGE Mission

L. Natalucci^a, M. Feroci^a, E. Quadrini^b, P. Ubertini^a, L. Piro^a, J.W. den Herder^c, D. Barret^d,
L. Amati^e, C. Budtz-Jorgensen^f, E. Caroli^e, S. Di Cosimo^a, M. Frutti^a, C. Labanti^e,
F. Monzani^g, J.M. Poulsen^g, L. Nicolini^g, A. Stevoli^g

^aINAF-Istituto di Astrofisica Spaziale e Fisica Cosmica, Sezione di Roma, via Fosso del Cavaliere 100, 00133 Roma, Italy;

^bINAF-Istituto di Astrofisica Spaziale e Fisica Cosmica, Sezione di Milano, Via E. Bassini 15, 20133 Milano, Italy;

^cSRON Netherlands Institute for Space Research, Sorbonnelaan 2, 3584 CA Utrecht, The Netherlands

^dCentre d'Etude Spatiale des Rayonnements, 9, avenue du Colonel Roche - BP 4346 31028 Toulouse Cedex 4, Toulouse, France

^eINAF-Istituto di Astrofisica Spaziale e Fisica Cosmica, Sezione di Bologna, via Gobetti 101, 40129 Bologna, Italy

^fDanish Space Research Institute, Juliane Maries Vej 30, DK-2100 Copenhagen, Denmark

^gThales Alenia Space, Strada Padana Superiore 290, 20090 Vimodrone, Italy

ABSTRACT

The success of the SWIFT/BAT and INTEGRAL missions has definitely opened a new window for follow-up and deep study of the transient gamma-ray sky. This now appears as the access key to important progresses in the area of cosmological research and deep understanding of the physics of compact objects. To detect in near real-time explosive events like Gamma-Ray bursts, thermonuclear flashes from Neutron Stars and other types of X-ray outbursts we have developed a concept for a wide-field gamma-ray coded mask instrument working in the range 8-200 keV, having a sensitivity of $0.4 \text{ ph cm}^{-2} \text{ s}^{-1}$ in 1 s (15-150 keV) and arcmin location accuracy over a sky region as wide as 3 sr. This scientific requirement can be achieved by means of two large area, high spatial resolution CZT detection planes made of arrays of relatively large ($\sim 1 \text{ cm}^2$) crystals, which are in turn read out as matrices of smaller pixels. To achieve such a wide Field-Of-View the two units can be placed at the sides of a S/C platform serving a payload with a complex of powerful X-ray instruments, as designed for the EDGE mission. The two units will be equipped with powerful signal read out system and data handling electronics, providing accurate on-board reconstruction of the source positions for fast, autonomous target acquisition by the X-ray telescopes.

Keywords: Gamma-ray telescopes, Gamma-ray detectors, Cadmium Zinc Telluride

1. INTRODUCTION

The relevance of X- and γ -ray broadband instrumentation has been largely established during the last decade, for the study of thermal and non-thermal physical processes in astrophysical sites, as well as their tight interaction spanning a very broad region of the electromagnetic spectrum (from the keV to the TeV range). Still very difficult remain the investigations of transient phenomena mainly due to the need of fast follow up. The sensitivity of wide field telescopes is intrinsically worse than what is needed for dedicated, sophisticated spectroscopy measurements and the time scale of the events to be studied is often in the range of seconds or minutes. Especially after the results of BeppoSAX (Boella et al, 1987) and SWIFT (Gehrels et al. 2004), it is recognized

Further author information: (Send correspondence to L.Natalucci)

L.Natalucci: E-mail: Lorenzo.Natalucci@iasf-roma.inaf.it, Telephone: +39 06 4993 4461

that important achievements can be obtained by short-term reaction to transient events like Gamma-Ray Bursts (GRBs), outbursts from compact objects and thermonuclear flashes from accreting Neutron Stars (NS).

Despite these phenomena have been known for long, new types of transient sources are appearing in most recent years. Among them, the Supergiant Fast X-ray Transients are a new class showing hour-long, hard X-ray outbursts (Sguera et al. 2006). These are accreting objects associated to High Mass X-ray Binaries with a Supergiant companion. Their growing number (despite the difficulty of detecting them) is suggesting they are a dominant class of binaries in our Galaxy, very interesting as they could be the progenitors of double NS binaries or NS/Black Hole binaries. Other recent, interesting class is that of Anomalous X-ray Pulsars (AXP), which have been discovered to undergo short, extremely hard outbursts (Kaspi 2007, Sguera et al. 2007).

Flaring behaviour of Galactic compact sources at time scales of hours to min is, therefore, a rather established but poorly studied phenomenon. Other fast and strong events have been found in Black Hole (BH) systems, like rapid flux variability of V4641 SGR (e.g. Wijnands & Van der klij 2000) and possibly GRB 070610, likely to be associated to a stellar black hole (Kasliwal et al. 2007). We also list giant outbursts of Cyg X-1 (Golenetskii et al. 2003) and bright flares from XTE J1650-500 (Tomsick et al 2003). These are probably not related to disk instability but can be interpreted in many ways, as violent activity of the inner accretion disk (e.g. feeding of material into jets), fluctuations of direct wind accretion, presence of thick, possibly clumpy absorbers or outflows. High resolution spectroscopy of these bright transient events is therefore a tool for important diagnostics, as well as for persistent X-ray emission. In accreting stellar Black Holes, the detection of Fe fluorescence lines with skewed profile can be explained by relativistic effects at the inner edge of accretion disk. On the other hand, broad and narrow Fe lines have been observed from Cyg X-1 while the source was in its intermediate state, which may be interpreted as originating from reflection on both inner region and disk (Miller et al. 2004).

Fine X-ray spectroscopy is also of key importance in the study of NS. The measurement of the gravitational redshift in observations of X-ray bursts, through detection of redshifted lines can lead to determination of the NS mass-radius relationship, hence constraining the equation of state of the dense nuclear matter. An important class of thermonuclear bursts are the superbursts, i.e. very long (\sim hours) events due to unstable burning of carbon and/or other products of the hydrogen/helium burning occurring on the NS surface. Despite these events are \sim 1000 times more energetic than normal type-I bursts, only a few of them are known, while it is very important to study their frequency and characteristics as a function of accretion rate (see e.g. Sthromayer & Bildsten 2003). Discrete components by Fe have been found in the spectrum of a superburst by 4U1820-30 (Sthromayer & Brown 2002).

We have developed a concept for an instrument exploiting a very wide region of the sky, to serve as an affordable, sensitive and moderate resource consuming payload complement for re-pointing capability in a fast-slewing satellite. The former success of the BeppoSAX/WFC (Jager et al. 1997) in the study of GRB and transient sources has motivated us to develop similar concept where source positioning is obtained by the use of coded masks, proven to be very successful also in the case of SWIFT and INTEGRAL (Winkler et al. 2003). This study, as reported hereafter has been targeted to the EDGE satellite (den Herder et al. 2007), to be flown on Low Earth Orbit (LEO). EDGE is a proposal for a class-M mission in the framework of the ESA Cosmic Vision Programme and carries a payload complex consisting of powerful X-ray spectroscopy and imaging telescopes, a Wide Field Monitor (WFM, described in this work) and a GRB detector.

EDGE looks as the ideal mission to exploit the above type of transient phenomena. Rapid response to X-ray transient events and capability of high resolution spectroscopy are the key to probe the extreme relativistic regime of the inner regions in BH accretion disks and physical conditions at the neutron star surface, e.g. by detection of line features in superbursts. In such a way the phenomena currently observed sporadically will be upgraded to real classes allowing to more detailed and well constrained models.

For an overview of the EDGE scientific objectives and payload see den Herder et al. (2007).

2. DESIGN OVERVIEW

The proposed design is based on the positioning of two identical units onto a payload module platform. The two cameras together are covering a region of the sky centered on the satellite pointing axis and are placed at opposite sides of a narrow field instrument complex. The composition of the FOVs of the two cameras and the

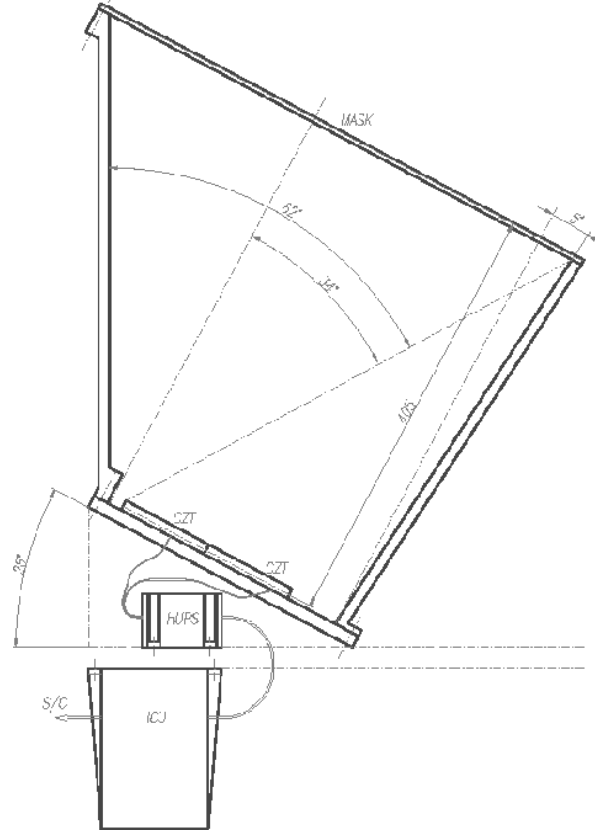


Figure 1. Design overview of one WFM camera (side view). The unit has the detector plane and mask plane inclined by 28 degrees respect to the S/C pointing axis. The vertical panel on the left is on the internal side (close to the X-ray telescope complex) while the oblique panel on the right is on the external side of the PLM structure, close to the radiator. The Instrument Control Unit is placed below the Payload Module plane, and provides the power to the detectors via the HVPS box.

large area of the detectors will ensure proper monitoring of a sky region as large as ~ 3 sr. Each WFM camera is complemented by a separate scintillator instrument for high energy extension (up to ~ 1 MeV).

As baseline detector type we have chosen CdZnTe (CZT), mainly due to its well-proven technology and excellent behaviour in space. Alternative solutions have been considered as the use of Silicon Drift devices coupled to CsI (Marisaldi & Labanti, 2004) and now regarded as possibly improved configuration awaiting further development in the next years. CZT detector technology is under development in Italy with a dedicated research and development program (Quadrini et al. 2007) as well as in many other european countries.

In figure 1 the baseline design scheme is described for a single camera (side view). The Wide-Field-Monitor (WFM) camera consists of one detection plane and one mask plane both inclined by an angle of 28 degrees from the S/C vertical axis (which is coincident with the viewing direction of the X-ray telescopes). The overall shape of the camera is not regular, for ease of payload accomodation (see Fig. 2). For the coded mask all the available space has been exploited, whereas the detector size is basically dictated by mass and power budget limitations. Detector and mask are separated by a distance of 40.5 cm, allowing for a source location accuracy of ~ 4 arcmin to be reached for objects brighter than $\sim 10 \sigma$ (see Sect. 3.1 for more details).

The geometric area of the detection plane is approximately 1410 cm^2 , to ensure an active area of 1340 cm^2 (the geometric area depends on the final detector design, mounting, thermal constraints etc.) and the energy range is such to cover effectively a wide band (8-200 keV). The inclination angle is chosen such as to ensure both a large aperture FOV and good matching with the payload allocation constraints. The unit is passively shielded

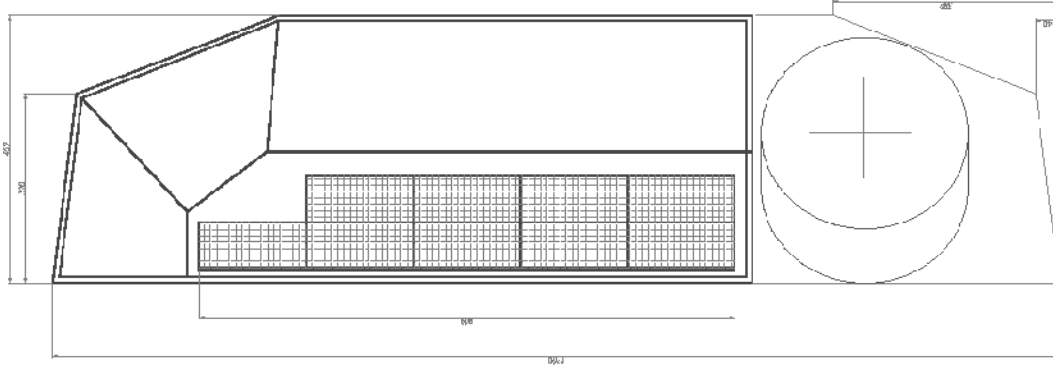


Figure 2. Design overview of one WFM camera (top view). A total of 9 CZT modules are assembled in two lines: 5 on the internal side and 4 on the external side. The large irregular polygonal shape represents the mask pattern placed at 40.5cm from detection plane, and connected to the bottom plane by side panels which are acting as a passive shield. The red cylinder at the right is the GRB detector. All dimensions are related to the projection on the S/C PLM plane (note that the camera is inclined by 28 degrees).

on all sides but the mask aperture, and sustained as a whole on the PLM platform by means of dedicated support. The shield is obtained by assembly of 5 side panels on which the coded mask support is fixed (by means of anchor bolts) and by one bottom shield placed under the CZT plane. No other collimating devices are present. Since the main source of background rate is the diffuse cosmic radiation, there is no real need for active anti-coincidence parts, thus allowing considerable weight saving. The shield units will be obtained by connecting one or two panels made of W and/or graded shield material, to be glued onto a CFRP sandwich and reinforced by additional grid structure.

A breakdown of the WFM components is graphically summarized in Fig. 3.

3. CZT ARRAY DETECTOR

CdZnTe are room temperature, semiconductor devices showing very good performance in terms of detector efficiency, spectral resolution and broad band coverage. The photon interaction cross section is dominated by photoelectric absorption up to ~ 200 keV. CZT crystals can be produced in large number and are also suitable to be assembled and integrated to form large area, pixellated detectors. These can be designed with a large variety of size, thicknesses, and array dimensions.

The electrical design of the detector is crucial to determine its performance. Due to the poor mobility of holes in the crystal compared to that of electrons, the signal amplitude will depend on the depth of the energy deposition site. This charge loss can be reconstructed to evaluate correctly the energy deposition, by recording and analysing the signal shape. Moreover the use of segmented electrodes (so-called "small pixel" configuration) causes the contribution of holes to the total charge collection to be much reduced, making the signal amplitude less dependent on the interaction depth. This technique is being studied through development of prototypes, including powerful FPGA based digital processing unit for events time sorting, electronic noise reduction, measurement of signal shape parameters (see Quadrini et al. 2007).

3.1 Detector design

The detection plane of a single camera is formed by the assembly of 9 identical modules, each of $18 \times 9 \text{ cm}^2$ (the size is approximated, being slightly dependent on the final number of pixels that can be achieved) mounted as shown in Fig. 4. Each module consists of one array of 16×8 CdZnTe square crystals with lateral size 10.8mm. As baseline, the thickness is at least 2mm (the CZT thickness can be easily selected from 1 to 10mm as function of the desired energy range and weight budget considerations). In turn, each crystal is read out as an array of smaller pixels. First prototypes foresee crystals divided in matrix of 4×4 and 16×16 pixels, each one with its own readout chain. As baseline, we will consider the basic crystal to be read out as 4×4 . This yields a pixel pitch of 2.7mm

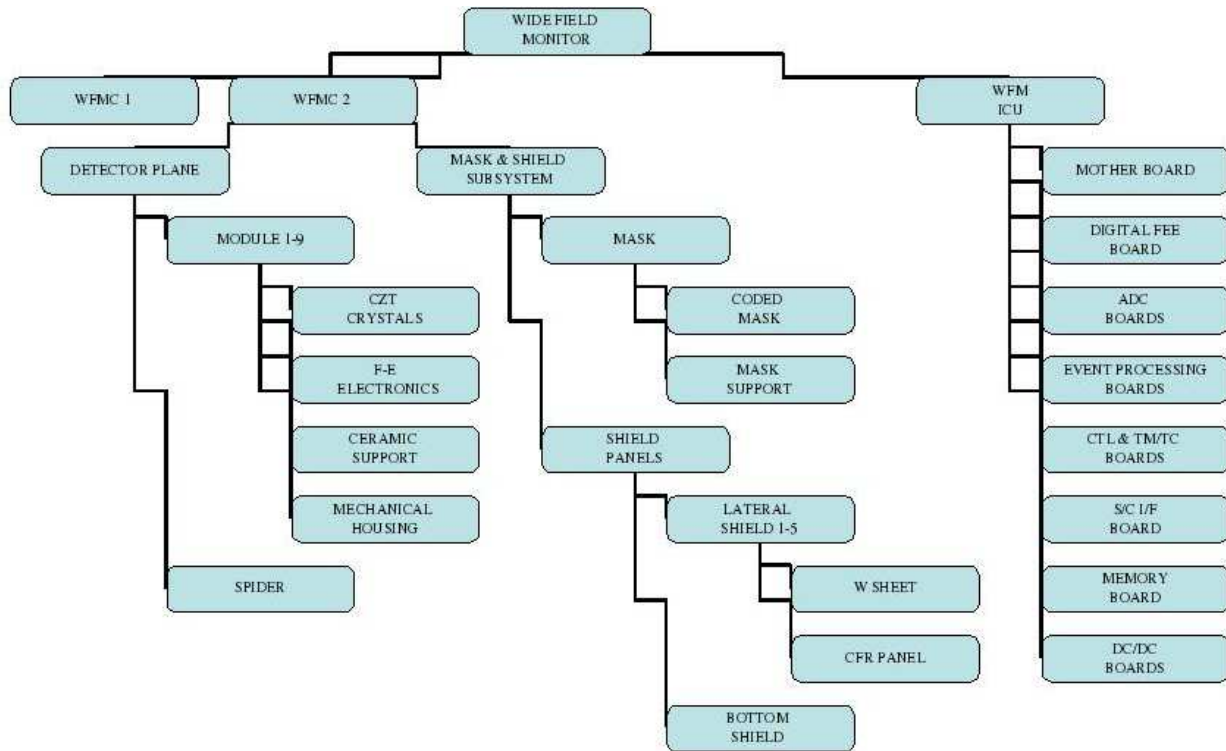


Figure 3. The WFM hardware tree showing the different subsystems.

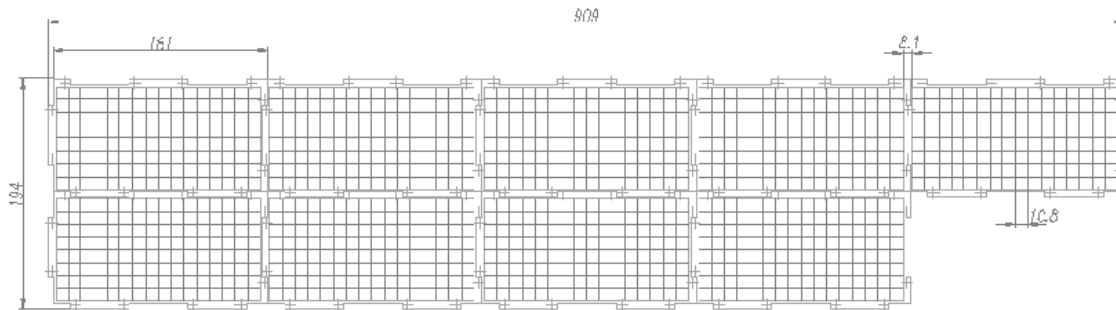


Figure 4. Schematic of detector assembly for one WFM unit (9 modules, 156 cm² each). Small red squares are the CZT crystals. Each crystal is in turn divided into 4x4 pixels.

and a total of $(4 \times 4) \times 8 \times 16 = 2048$ pixels/module, i.e. 18432 pixels for each camera. This choice implies an angular resolution of about 35 arcmin for a mask placed at a distance of 40.5cm. Potentially a finer sub-division (16 x 16 pixels) is also feasible at the expense of additional power and complexity. This choice is considered a reasonable compromise between available power budget and location accuracy requirement, however the baseline may be hopefully changed if new technological achievements will make possible to increase the detector spatial resolution e.g. by a factor 2 within reasonable power budget. The development of low power ASICs for space application is promising. Prototypes to be used with other semiconductor (GaAs) detectors show power consumptions as low as 0.8 mW/ch (Bastia et al. 2006). These have already been manufactured and tested and we are presently considering the possibility of customizing this chip for application to CZT detector prototype to be built in the near future.

In the current design the FEE is made of 32x32 ASIC readout system, with 2 ASICs/module mounted below the CZT and within the spider acting as detector support. The space between detection plane and S/C PLM

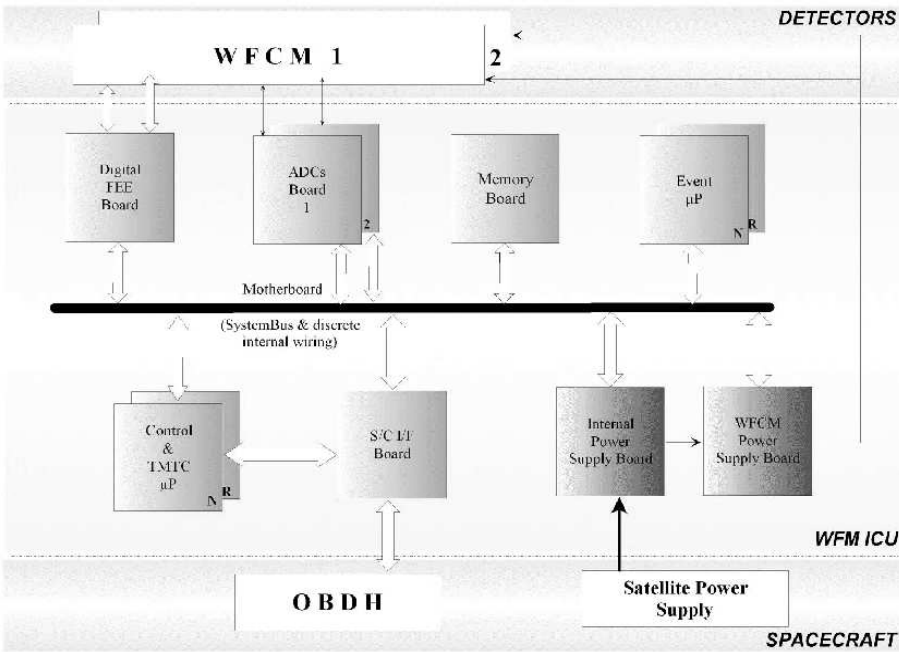


Figure 5. Instrument Control Unit (ICU) functional block diagram. The S/C interfaces for both data/commands and power supply are also indicated.

plane can be used to host also the HVPS units for the detector modules. Single crystals are mounted within egg-crate cells hosting 4x4 crystals each (8 cells/module) as shown in Fig. 1. Each module is in turn controlled by the DFEE for signal acquisition and conditioning, performing ADC conversion, background rejection and event reconstruction. Most applications will be implemented in the Instrument Control Unit (ICU, see below).

As a baseline, each module will be protected by a thin cover for optical light rejection. A thermal blanket for the mask can be foreseen in case of threshold energy higher than ~ 7 keV. If the lower level threshold has to be reduced, this blanket may have to be replaced by a removable cover.

4. INSTRUMENT CONTROL UNIT

A single ICU serving both WFM cameras controls the S/C interface, TM/TC and provides the processing for trigger, validation and positioning of γ -ray transient events using data from both cameras (in Fig. 5 is shown a functional diagram) and from the GRB detector. The WFM ICU houses a total of 12 boards, two of which are redundant microprocessor units.

The ICU is mounted below the PLM plane as shown schematically in Fig. 1. Its approximate size is $26 \times 32 \times 20$ cm³. In Fig. 5 is shown the functional diagram with the ICU components and I/Fs, as well as identification of the tasks performed.

Data compression and handling of the different operating modes will be performed to ensure smooth operations and reliable trigger mechanism. This will be based on the elaboration of count rates on different time scales and energy intervals from different detector sections. A coincidence with the GRB detector (possibly via the S/C interface) will be normally required, to avoid the largest possible number of false triggers. The source positioning will be obtained by flat-fielding, cross-correlation and peak search methods. Criteria for source validation and selection will be defined by dedicated future study. This will take advantage in particular, from the expertise in the development of the GRB alert and fast localization procedures on board the AGILE satellite (Tavani et al. 2006).

5. RESOURCE BUDGETS

The mass and power resources needed by the WFM have been evaluated. The weight for each WFM camera is approximately 51 kg, shared between detector (~ 19 kg), mask (~ 10 kg) and shield (~ 22 kg). Adding 8 kg to

Table 1. Instrument performance parameters vs design requirements. The "model" column represents the actual performance of the baseline configuration of the WFM.

Parameter	Requirement	Model	Goal	Comment
Energy Range (keV)	8-200	8-200	5-200	Region with on axis effective area > 20% of max.
Field-Of-View	2.5 sr	2.5 sr	3 sr	Region with average effective area > 300 cm ²
Energy Resolution	5%	3%	3%	Values at 100 keV
Effective Area 10-100 keV	1000 cm ²	1100 cm ²	1200 cm ²	Determined on S/C pointing axis
Angular Resolution	35 arcmin	34 arcmin	18 arcmin	FWHM resolution
Location Accuracy	4 arcmin	4 arcmin	2 arcmin	SNR > 10 σ
Time Resolution	10 ms	10 μ s	10 μ s	
Max. Count Rate	5000 c/s	5000 c/s	5000 c/s	Max. value estimated for Galactic Plane in FOV
S/W Processing Time	20 s	< 20 s	5 s	Time necessary for burst localization
Continuum Sensitivity (ph cm ⁻² s ⁻¹)	0.5	0.4	0.4	15-150 keV band, 1s integration time

be allocated for the ICU the total instrument weight is 111 kg (133 kg including 20% contingency). The total power, as primary line at S/C level is estimated to be approximately 127 W (140 kg with 10% contingency) by using a basic figure of 1.2 mW/channel.

The long time averaged data production rate is dominated by the count rate intensity when observing with the Galactic Plane in the FOV (up to 5000 c/s per camera). Data are stored on board each orbit and then transmitted. In case no onboard data selection or compression scheme are considered, and assuming that 10% of the time is available for download (9 min out of 90 min orbit period) the total telemetry demand is estimated to be ~ 5 Mbits/s. In case the threshold is lowered to e.g 5 keV or less the count rate will increase by about a factor two. The above estimated value is at least a factor 3 more demanding than the current limit requirement of 1.5 Mbits/s (based on a total data rate of 5 Mbits/s for the whole EDGE mission). Therefore it is foreseen that at least part of the data will be not transmitted as photon by photon but histogrammed on board. In this case, it is required to extend the event processing and background rejection capability, as implemented in the ICU.

6. PERFORMANCE PREDICTION

In figure 6 is shown the effective area of the WFM for a source in the direction coincident with the satellite pointing. This includes the area projections, the total detection efficiency and mask transparency and open fraction (assumed 50%) as well as the efficiency loss due to image reconstruction (finite spatial resolution of detection plane).

For the purpose of the WFM however, an important performance issue is how the effective area changes with varying offset direction. To evaluate the capability of the WFM to detect a source in a large enough FOV, we compute the average exposed area for sources shining at a given offset angle respect to the S/C pointing direction. The average is computed along a circle corresponding to the offset. This is obtained by composition of the two FOVs related to the two different cameras. The plot in Fig. 7 shows that the effective area exposed to a source within 2.5 sr is always greater than 300 cm², which is evaluated as the limit to detect bursts with fluences higher than 10⁻⁶ erg/cm² (the lower limit requirement for bright GRBs). For bursts brighter than two times this limit the useful region increases to 3.7 sr.

The sensitivity of the WFM in the 10-200 keV region is very similar to the INTEGRAL/IBIS one. Below 100 keV it is estimated as 2-3 mCrab in 10⁵s, which translates to ~ 1 Crab in 1 sec (the sensitivity vs short events is most relevant for the WFM). In summary the instrument will have a sensitivity similar to IBIS/ISGRI with an expected improvement for E > 150 keV, due to the better background conditions in low earth orbit.

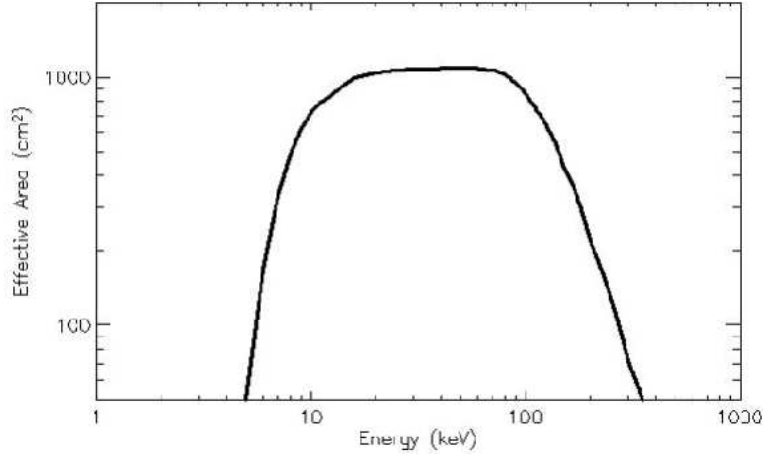


Figure 6. On axis effective area of the Wide-Field-Monitor. It includes contribution from both cameras and refers to a direction coincident with the S/C viewing axis.

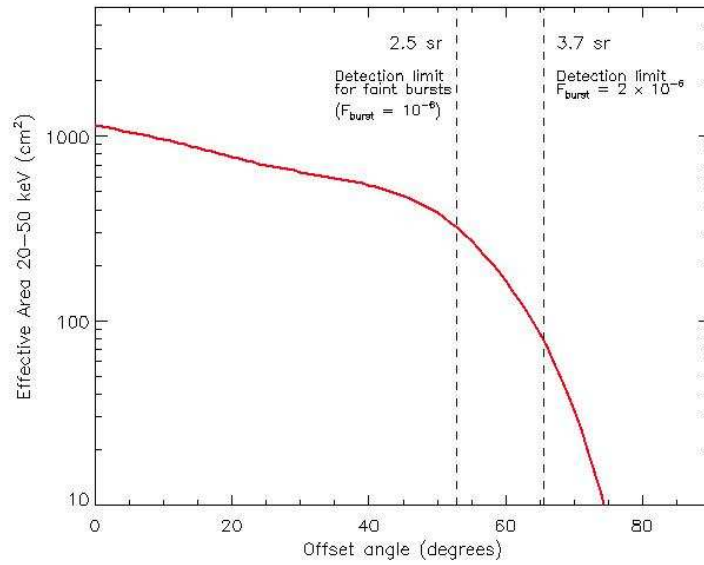


Figure 7. The effective area of the two WFM units, shown versus the offset angle to the S/C pointing axis. Indicated by the dashed lines are the offset values, corresponding to the minimum effective area needed to detect bursts with fluences of 10^{-6} erg/cm² and 2×10^{-6} erg/cm². The fluence limit for faint GRBs corresponds to the design requirement of the EDGE mission for the detection of GRBs for the WHIM studies.

In Table I we report the basic performance parameter as evaluated today, compared to the performance requirements of the EDGE mission.

REFERENCES

1. Bastia, P., Bertuccio, G., Borghetti, F. et al., "A complete Read-Out ASIC for Use with large Pixel X-ray Detector Array", ESA-SP 630, p.28, 2006
2. Boella, G., Butler, R. C., Perola, G. C. et al., "BeppoSAX, the wide band mission for X-ray astronomy", A&A Suppl., 122, 299, 1997
3. den Herder, J.W., Piro, L., Ohashi, T. et al., "EDGE: Explorer of Diffuse Emission and Gamma-ray Burst Explosions", these Proceedings, Conf. 6688, 2007

4. Gehrels, N., Chincarini, G., Giommi, P. et al., "The SWIFT Gamma-Ray Burst Mission", *ApJ* 611, 1005, 2004
5. Golenetskii, S., Aptekar, R., Frederiks, D., Mazets, E., Palshin, V., "Observations of Giant Outbursts from Cygnus X-1", *ApJ* 596, 1113, 2003
6. Jager, R., Mels, W. A., Brinkman, A. C., et al., "The Wide Field Cameras onboard the BeppoSAX X-ray Astronomy Satellite", *A&A* 125, 557, 1997
7. Kasliwal, M.M., Cenko, S.B., Kulkarni, S.R. et al., "GRB070610: A Curious Galactic Transient" *ApJ* submitted, arXiv:0708.0226v1 [astro-ph], 2007
8. Kaspi, V.M., "Recent Progress on Anomalous X-ray Pulsars", *Astrophysics & Space Science*, Vol. 308, No. 1-4, p.1, 2007
9. Marisaldi, M., Labanti, C., Bulgarelli, A. et al., "A Position Sensitive Gamma-Ray Detector Based on Silicon Drift Detectors Coupled to Scintillators for Application in the MEGA Compton Telescope", *Proc. IEEE NSS Conf.*, 2004
10. Miller, J.M., Raymond, J., Fabian, A.C. et al., "Chandra/High Energy Transmission Grating Spectrometer Spectroscopy of the Galactic Black Hole GX 339-4: A Relativistic Iron Emission Line and Evidence for a Seyfert-like Warm Absorber", *ApJ* 601, 450, 2004
11. Quadrini, E.M, Uslenghi, M., Alderighi, M. et al., "Spectroscopic CZT detectors development for X and Gamma-Ray Imaging Instruments", these Proceedings, *Conf. 6686*, 2007
12. Sguera, V., Bazzano, A., Bird, A.J. et al., "Unveiling Supergiant Fast X-Ray Transient Sources with INTEGRAL", *ApJ* 646, 452, 2006
13. Sguera, V., Bazzano, A., Bird, A.J. et al., "INTEGRAL high energy detection of the transient IGR J11321-5311", *A&A*, in press, arXiv:0704.2737v1 [astro-ph], 2007
14. Strohmayer, T.E & Bildsten, L., "New views of thermonuclear bursts", in "Compact Stellar X-ray Sources", eds. W.H.G. Lewin and M. van der Klis, Cambridge, Cambridge University Press, 2003
15. Strohmayer, T.E., & Brown, E.F., "A Remarkable 3 Hour Thermonuclear Burst from 4U 1820-30", *ApJ* 566, 1045, 2002
16. Tavani, M., Barbiellini, G., Argan, A., "The AGILE Mission and its Scientific Instruments", *Proc. SPIE* 2006, vol. 6266, 2006
17. Tomsick, J.A., Kalemci, E., Corbel, S., Kaaret, P., "X-Ray Flares and Oscillations from the Black Hole Candidate X-Ray Transient XTE J1650-500 at Low Luminosity", *ApJ* 592, 1100, 2003
18. Wijnands, R. & Van der Klis, M., "The Rapid X-Ray Variability of V4641 Sagittarii (SAX J1819.3-2525 = XTE J1819-254)", *ApJ* 528, L93, 2000
19. Winkler, C., Courvoisier, T. J-L., Di Cocco, G. et al., "The INTEGRAL Mission" *A&A* 411, L1, 2003